Environmental Research 229 (2023) 115896

Contents lists available at ScienceDirect

Environmental Research

journal homepage: www.elsevier.com/locate/envres

Predicting highly dynamic traffic noise using rotating mobile monitoring and machine learning method

Yuyang Zhang [a], Huimin Zhao [b], Yan Li [b,*], Ying Long [b], Weinan Liang [a]

[a] Department of Urban Planning and Landscape, North China University of Technology, Beijing, 100144, China
[b] School of Architecture, Tsinghua University, Beijing, 100084, China

ARTICLE INFO

Handling Editor: Aijie Wang

Keywords:
Dynamic traffic noise
Rotating mobile monitoring method (RMM method)
Noise prediction
Noise map

ABSTRACT

Traffic noise, characterized by its highly fluctuating nature, is the second biggest environmental problem in the world. Highly dynamic noise maps are indispensable for managing traffic noise pollution, but two key difficulties exist in generating these maps: the lack of large amounts of fine-scale noise monitoring data and the ability to predict noise levels in the absence of noise monitoring data. This study proposed a new noise monitoring method, the Rotating Mobile Monitoring method, that combines the advantages of stationary and mobile monitoring methods and expands the spatial extent and temporal resolution of noise data. A monitoring campaign was conducted in the Haidian District of Beijing, covering 54.79 km of roads and a total area of 22.15 km^2, and gathered 18,213 A-weighted equivalent noise (LAeq) measurements at 1-s intervals from 152 stationary sampling sites. Additionally, street view images, meteorological data and built environment data were collected from all roads and stationary sites. Using computer vision and GIS analysis tools, 49 predictor variables were measured in four categories, including microscopic traffic composition, street form, land use and meteorology. Six machine learning models and linear regression models were trained to predict LAeq, with random forest performing the best ($R^2 = 0.72$, RMSE = 3.28 dB), followed by K-nearest neighbors regression ($R^2 = 0.66$, RMSE = 3.43 dB). The optimal random forest model identified distance to the major road, tree view index, and the maximum field of view index of cars in the last 3 s as the top three contributors. Finally, the model was applied to generate a 9-day traffic noise map of the study area at both the point and street levels. The study is easily replicable and can be extended to a larger spatial scale to obtain highly dynamic noise maps.

1. Introduction

Frequent exposure to high levels of noise can lead to physical and psychological problems in residents such as hearing impairment (Wang et al., 2021), cardiovascular disease (Begou et al., 2020; Zhang et al., 2023), type 2 diabetes (Sørensen et al., 2022), irritability (Paiva et al., 2019), anxiety (Lan et al., 2020), and poor mental health (Klompmaker et al., 2019). In addition, noise has been shown to be associated with a decrease in biodiversity (Halfwerk et al., 2011). With rapid urbanization, complex urban road networks and dense traffic flows make traffic noise the most dominant type of noise (Thakre et al., 2020) and the second most important environmental problem (Morel et al., 2012; Shukla et al., 2012). Traffic noise is featured by its highly fluctuating nature and the construction of highly dynamic noise maps can be used to assess and effectively manage traffic noise pollution. However, there are two main challenges in constructing noise maps, including acquiring large amounts of noise monitoring data with both fine-level spatial and temporal resolution as well as predicting dynamic noise levels without noise monitoring data (Lan and Cai, 2021).

Noise monitoring can be done through stationary or mobile methods. Stationary noise monitoring stations provide accurate noise data with high temporal resolution (Mioduszewski et al., 2011; Zambon et al., 2018), but have limited spatial coverage due to high construction and maintenance costs (Monti et al., 2020). In contrast, mobile monitoring that performed by researchers on bicycles (Quintero et al., 2021; Quintero et al., 2019) or on foot (Guillaume et al., 2019), carrying professional sensors (Quintero et al., 2021; Quintero et al., 2019) or smartphones (Leao et al., 2014; Zappatore et al., 2016), provides higher spatial resolution but lower temporal resolution due to short stay periods while constantly moving. In addition, the movement speed of data collectors is generally low because the noise generated by high-speed movements affects the accuracy of the data (Guillaume et al., 2019),

* Corresponding author.
E-mail address: yanli427@hotmail.com (Y. Li).

https://doi.org/10.1016/j.envres.2023.115896
Received 12 January 2023; Received in revised form 2 April 2023; Accepted 11 April 2023
Available online 11 April 2023

which means that it is more time-consuming and labor-intensive to achieve monitoring over large geographical areas. Recently, smartphones have widened the scenarios of mobile monitoring due to their high occupancy. Several mobile applications supporting noise monitoring have emerged, e.g., Noisespy (Kanjo, 2010), NoiseProbe (Ghosh et al., 2019), but the accuracy of noise data acquired by cell phones is still far lower than that of professional sensors (Lu et al., 2009). Therefore, it is essential to develop an effective monitoring method that could acquire precise noise data with both high temporal and spatial resolution.

For predicting noise levels, predictor variables can be basically categorized into four types: traffic composition, street form, land use, and meteorology, which essentially represent noise sources and noise transmission (Garg and Maji, 2014; Nijland and Van Wee, 2005). While street form, land use and meteorological variables are static, traffic composition variables are dynamic and considered the dominant traffic noise sources. Microscopic traffic flow characteristics, such as the number of vehicles and pedestrians passing per second, are more relevant to dynamic traffic noise and can be identified through visual images. High coverage open-source street view images (Kang et al., 2020; Anguelov et al., 2010) and road surveillance videos (Sun et al., 2022) provide potential data for prediction. For example, Ibili and Owolabi (2019) collected traffic flow data and speed data from a digital video recorder, while Thakre et al. (2020) used a digital camera Fujifilm Finepix S3300. However, these studies have manually calculated these microscopic traffic composition variables, resulting in limited samples and labor-intensive work. Image-based deep learning models, such as segmentation and object detection, provide automatic analysis tools for extracting traffic information from images (Gebru et al., 2017; Yan and Ryu, 2021; Sun et al., 2022).

In addition, several studies in recent years have demonstrated the advantages of machine learning models, such as neural networks (NNs), extreme gradient boosting (XGB), in noise prediction (Genaro et al., 2010; Yin et al., 2020; Fallah-Shorshani et al., 2022). However, most studies (Ryu et al., 2017; Chang et al., 2019) still use statistical and land use regression methods, ignoring the complex nonlinear relationships and interactions among the predictor variables.

In summary, there are still three significant gaps in existing studies, including 1) current monitoring methods have limitations in generating accurate large-scale dynamic noise maps requires noise monitoring data with high spatial and temporal resolution; 2) microscopic traffic composition variables that change rapidly over time, have not been measured in large samples, such as numbers of vehicles and people present at a given location and time; 3) the complex relationships between predictor variables and traffic noise are not adequately considered in the construction of noise prediction models.

In view of this, this study aims to construct high-precision dynamic noise maps over a large geographical area. Firstly, this study developed a new noise monitoring method called Rotating Mobile Monitoring method (RMM), which combines the advantages of stationary and mobile monitoring methods to achieve the collection of high precision noise data with high spatial and temporal resolution, but with less human labor and time to acquire. Secondly, along with the noise data, video data and meteorological data were collected and processed to measure microscopic traffic composition and meteorological variables, respectively. Thirdly, machine learning methods were applied to achieve fast data processing and accurate prediction model construction. Finally, traffic noise mapping was completed with high accuracy and full spatial coverage.

2. Materials and methods

The overall methodology proposed for the traffic noise monitoring, modelling and prediction in this study has been shown in Fig. 1, including five procedures: variable selection, data retrieval, variable measurement, noise prediction modeling and traffic noise mapping.

2.1. Study area

As the capital and second largest city in China, Beijing has high-dense road networks and heavy traffic volumes, producing serious traffic noise pollution. Our study area is located in the Haidian district of Beijing, covering four townships of Qinghuayuan, Zhongguancun, Yanyuan and Shuangyushu. Within this area, there is a wide mixture of urban land use, including core commercial areas (urban sub-centers), top-ranked universities, residential communities, parks, as well as roads of different grades (Fig. 2). The total area is 22.15 km^2 and the total length of the research roads is 54.79 km.

2.2. Variable selection

The predictor variables included four categories: microscopic traffic composition, street form, land use and meteorology. The variables were initially selected based on a literature review (Table 1). Specifically, street form variables, such as greenspace provisions and building forms, reflect attenuation between noise source locations and receiver locations (Fallah-Shorshani et al., 2018). While other street form variables, including road width, distance to the junctions, and transportation facilities, could be served as noise sources (Lu et al., 2019; Fallah-Shorshani et al., 2018). Meteorological variables, such as air temperature

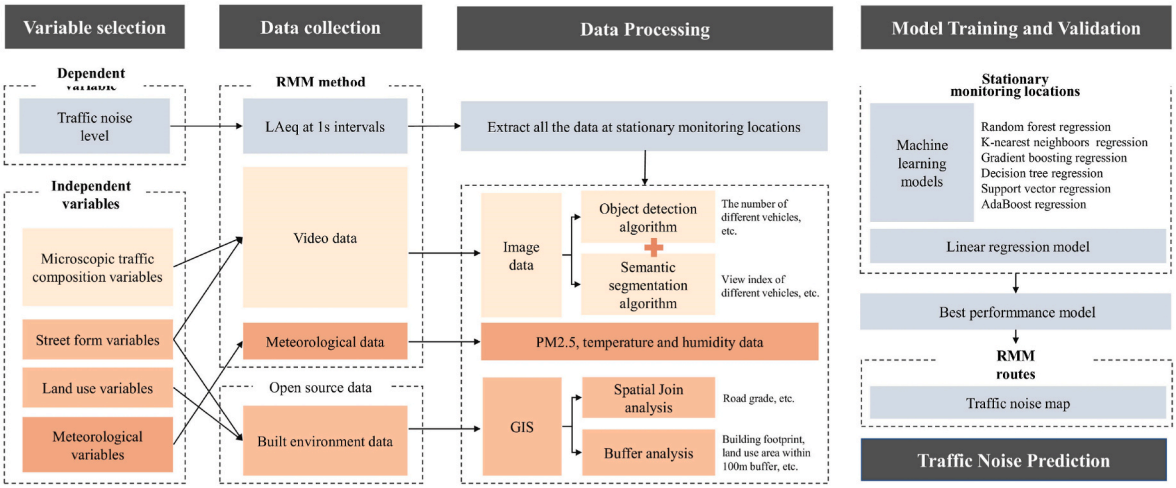

Fig. 1. Methodology.

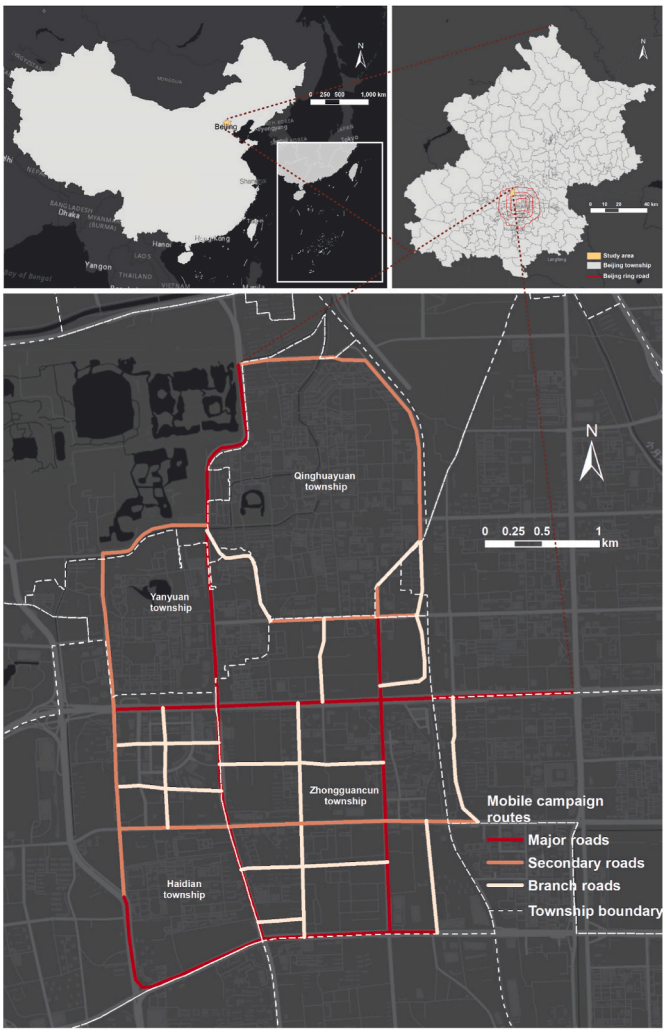

Fig. 2. Study area and grades of monitoring route.

and relative humidity, attenuate noise levels through atmospheric absorption (Liptai et al., 2015). Microscopic traffic simulations have incorporated vehicle counts as input to reveal the causal chain between traffic noise and road features in Dalian, China (Lu et al., 2019). Nourani et al.(2020) also predicted dynamic traffic noise in Nicosia, North Cypru using the number of various vehicles as a predictive variable.

The final list of variables was adjusted to better suit our research questions (Table 2). The differences from previous studies are stated as follows: first, considering that our study area is in an urban center with high population density, the noise caused by pedestrians cannot be ignored. Therefore, this study included the variables related to pedestrians as traffic composition variables. In addition to identifying numbers, this study also calculated view index variables in microscopic traffic composition category, including view indices of cars, trucks, buses, mopeds, bicycles and pedestrians, which can, to a certain extent, reflect the distance to these noise sources. Also, highest view indices in the last 3 s were chosen as variables to account for noise that may have reached the camera field of view before the vehicle appeared in the image. In the street form category, this study also added six view index variables, including view indices of sky, buildings, trees, grass, plants and fences. These variables reflect street form from the human eye's perspective, i.e., the human perception of the environment, and are also related to the attenuation of traffic noise. In the land use category, four types of land use, including residential communities, schools, urban parks and shopping malls and hotels, were selected, as they ranked highly in terms of size.

2.3. Data retrieval

2.3.1. RMM data

Compared to stationary monitoring method, the mobile monitoring method expands the spatial coverage but also has a limitation that the sampling time is extremely short at each sampling location. Therefore, this study proposed a new noise monitoring method called Rotating Mobile Monitoring (RMM) method, which was inspired by the work in Accra, Ghana (Clark et al., 2022). With highly spatially and temporally heterogeneous characteristics, the noise varies dramatically from time to time even at the same geographical location. To capture the spatial and temporal variation of A-weighted equivalent noise (LAeq in decibels, dB) and its sources per second across the study area, this study combined the advantages of stationary and mobile monitoring methods by rotating the stationary sampling sites during a mobile monitoring campaign. Mobile routes covered every street in the study area, and ArcMap's Find Shortest Path tool was used to calculate and obtain routes for navigation in each acquisition. The stationary sampling points were feature points in each street, representing a variety of urban characteristics, including narrow and wide roads, proximity and distance from intersections, sparse and dense built-up areas, and high and low proportions of green space. To enhance the spatial heterogeneity of noise, this study did not select the same sampling location every day. Finally, 152 stationary sampling locations were determined (Fig. 3).

For the sampling time, it is hard to achieve high spatial coverage in a short period of time if the sampling time for each location is too long. However, if the sampling time is too short (less than 30 s), it is also impossible to cover a wide range of traffic conditions. Therefore, for intersections equipped with traffic signals, it is necessary to wait at least one full round of signals from red to green, about 120 s. For other points on the street, it is necessary to stay 1–3 min at a time in order to cover the variation from free traffic conditions to busy traffic conditions. The mobile route and stationary sampling locations were presented in Fig. 3. The monitoring route was on the bike lane, about 2–3 m away from the pavement, and the sound of normal human conversation had no significant effect on the traffic noise.

During the RMM campaign, an electric bicycle (e-bike) was deployed to carry professional monitoring devices in order to monitor a large geographical area in a short time (Fig. 4). E-bikes have the advantages of being electric-motivated, meaning that no sound when being at still, no emissions, and an average speed of 20 km/h (a maximum speed of 35 km/h). A professional noise meter (Smart Sensor AR844) was used to collect LAeq noise data at 1-s intervals with a 1-s sampling frequency. The noise meter had a resolution of 0.1 dB, a measurement range of 30–130 dB, and an accuracy of ±1.5 dB. During data collection, the noise meter's microphone was always aimed at the road ahead and positioned away from the researcher's body to minimize any noise reflections. The researcher refrained from speaking to avoid distorting the accurate measurement of noise. Along with the noise meter, the e-bike was equipped with a GoPro 9 camera, which was also pointed ahead of the road and used to collect real-time street video data at 60 Hz, and a customized mobile meteorological station with a sampling frequency of 1 s, which was used to collect $PM_{2.5}$, air temperature and humidity. During each RMM period, the GoPro 9 and mobile meteorological station were sampling all the time to acquire street view images and meteorological conditions while moving and rotating fixed sampling points. The Footpath GPS recording application on the smartphone (iPhone 12 Pro Max) was also turned on to record the GPS tracks of the e-bike. The time of all the devices were synchronized with the smartphone to ensure that the timeline of the data collected by each device remains consistent.

This study was conducted over nine weekdays from July to August 2022, selecting only rain-free days. Data was collected every day from 12:00 to 16:00 before the evening rush hours. However, due to sudden rain on August 8th, the last 3 km of the route could not be completed, resulting in missing data for that section. In total, this study obtained a

Table 1
An overview of the variables used in previous studies.

Publication	Traffic composition	Street form	Meteorology
Fallah-Shorshani et al. (2018)	Average hourly traffic volume within various Euclidean buffers	Euclidean distance to the shore, to the closest airport, to the rail line, to the highway, to the nearest major road; building footprint area, areas of different types of land use (commercial, governmental and institutional, resource and industrial, parks, residential, open area, and water), lengths of different types roads (highway, major roads, local roads, and bus routes), numbers of intersections, bus stops, trees and chimneys, and the average and maximum building height within the Euclidean buffers	Distance to chimneys emitting Nitrogen Oxides or Particulate Matter.
Mansourkhaki et al. (2018)	Total traffic volume per hour, average speed of vehicles, percentage of each category of vehicles	Road gradient, density of buildings around the road section and building reflection factor	–
Ahmed and Pradhan (2019)	Number of different vehicles (cars, heavy vehicles, motorbikes) per 15 min, sum of vehicles and ratio of different vehicles (cars, heavy vehicles, motorbikes)	Highway density, digital surface model and digital elevation model	Wind speed
Quintero et al. (2019)	Number of light vehicles, medium heavy vehicles, heavy vehicles, and bikes passes-by, and traffic flow	Distance to the nearest cross street	
Chen et al. (2020)	Per-vehicle noise value, vehicle type (heavy vehicle, medium vehicle, light vehicle), and vehicle velocity	Roadway gradient	–
Thakre et al. (2020)	Number of different vehicles (light, medium, heavy vehicles) and number of honks	–	–
Yin et al. (2020)	Traffic volume, traffic density, and traffic speed	Length of different types roads (motorway, primary, secondary, tertiary, residential, service and others), the distance to nearest road, the numbers of intersections of different grades (major-major , major–minor; major - minor; major–branch), the numbers of traffic signals, area of different types of land use (residential, commercial, industrial, and park), building area, maximum building height and percent tree canopy within Euclidean buffers	Temperature, pressure, cloud cover, dew point, humidity, wind speed, wind direction, wind gust, and 12 other meteorological variables
Gilani and Mir (2021)	Traffic volume per hour (excluding the volume of heavy vehicles), average traffic speed, number of heavy vehicles and number of honking events per hour	Carriageway width	–

total of 18,213 LAeq data from 152 stationary sampling sites, 350 GB of video data and 80,998 meteorological data from 54.79 km of roads.

2.3.2. Built environment data

The road network data, land use data and building footprint data was all acquired form Gaode Map, one of the leading map service providers in China. The road network data for 2021 was provided in shapefile format (.shp) and included information on the length and width of major, secondary, and branch roads. This data was used to generate mobile routes, extract road grades and widths at monitoring points, and measure the distances from sampling points to intersections in order to improve our understanding of traffic noise patterns in the study area. The Area of Interest data from 2021 was used to represent land use patterns, which describe the specific boundaries of each type of land use, including residential areas, schools, parks and shopping centers. The building footprint data for 2021 (.shp) included building shapes and the number of floors, and was used to measure building footprint area and floor area ratio (FAR). The green space data was extracted from a 1.07 m spatial resolution Google Earth image as of September 18, 2020, as it shows distinct green space and less shading from buildings and trees.

2.4. Variable measurement

This study identified 49 traffic noise related variables, which can be categorized into four categories (Table 2). Regarding different data sources, 22 variables were extracted from video data, 9 from road network data, 8 from land use data, 4 from building footprint data, 2 from remote sensing data and 4 from meteorological data.

The video and meteorological data collected by RMM were used to measure microscopic traffic composition variables and meteorological variables, respectively, while built environment data were used to measure street form variables.

For microscopic traffic composition variables, video data were used to extract features using two computer vision methods – object detection and segmentation. First, videos were converted to frames at 1-s intervals using OpenCV-Python package, while the timestamp of each frame was inferred from the modification time of the video file that recorded the end time of the video. The coordinates of each frame were retrieved by concatenating them with the timestamps of GPS coordinates. Second, to identify the traffic around the sampling points, an object detection model was used to identify the number of pedestrians, bicycles, cars, motorcycles, buses, trains, trucks, stop signs and parking meters in each frame. The YOLOv7 model trained on MS COCO datasets from scratch presented in the paper (Wang et al., 2022) was used for detection with

Table 2
Summary of variables in this study.

Variables	Description	Data types	Method
Traffic composition variables			
Number of different vehicles (cars, trucks, buses and mopeds)	The number of corresponding objects in the image	Video data	Object detection algorithm
Number of pedestrians			
Number of stop signs			
Number of parking meters			
View index of different vehicles (cars, trucks, buses and mopeds)	View index of corresponding objects in the image		Semantic segmentation algorithm
Pedestrian view index			
Maximum view index of different vehicles (cars, trucks, buses and mopeds)	Maximum view index of different vehicles in the last 3 s		
Street form variables			
Road grade	Three grades: major, secondary and branch roads	Road network data	Spatial join tool in ArcMap 10.2
Road width	The width of the road		
Distance to the major road	The Euclidean distance from the sampling points to the major road		Proximity analysis tool in ArcMap 10.2
Distance to the intersections of different grades (major–major; major–secondary; major–branch; secondary- secondary; secondary-branch; branch-branch)	The Euclidean distance from the sampling points to the intersections		
Building density within Euclidean buffers (100m and 200m)	The area of the building footprint within Euclidean buffers	Building footprint data	Analysis tools in ArcMap 10.2
Floor area ratio (FAR) within Euclidean buffers (100m and 200m)	The area of the building floor area within Euclidean buffers		
Green area ratio within Euclidean buffers (100m and 200m)	The area of the green space within Euclidean buffers	Remote sensing data	K-Means clustering method in ENVI 5.3 and analysis tools in ArcMap 10.2
View index of built environment indicators (building, sky, tree, grass, plant, fence)	View index of corresponding objects in the image	Video data	Semantic segmentation algorithm
Land use variables			
Land areas of Residential communities, schools, urban parks, and shopping malls within Euclidean buffers (100m and 200m)	The area of the corresponding land use type within Euclidean buffers	AOI data	Analysis tools in ArcMap 10.2
Meteorological variables			
$PM_{2.5}$	Meteorological variables value at the moment of noise monitoring	Meteorological data	–
PM_{10}			
Temperature			
Humidity			

an average precision of 56.8%, outperforming all known object detectors in terms of speed and performance. Third, based on the assumption that objects have a distance effect, i.e., objects at close distances introduce larger noise, the view indices of objects were calculated to represent the distance, i.e., the closer the distance the larger the view index. A semantic segmentation approach with the DeepLab V3 model pre-trained on the MIT ADE20k datasets using Xception-65 as the base model was implemented in the Pixellib library to segment the aforementioned traffic objects and to calculate the percentage of the pixels classified as each object in the total image pixels. In addition, to discover the objects behind the collecting bicycle, the maximum view indices of different traffic objects in the last 3 s were calculated to represent the front-to-back noise around the monitoring points.

For street form variables, video, road network, building footprint and remote sensing data were used to measure these variables. The DeepLab V3 semantic segmentation model with the same parameters mentioned above was used to retrieve the view indices of the built environment components, including buildings, sky, trees, grasses, fences and plants. Meanwhile, ArcMap's spatial join tool was used to connect the sampling points and road network data. The grade and width information of the road where each point was located was assigned to that point. The Euclidean distance from the sampling points to the intersections of different levels were measured by proximity analysis tool in ArcMap 10.2. The K-Means clustering method in ENVI 5.3 was used to extract the green space vector data from the remote sensing images. Then, by referring previous studies (Chang et al., 2019; Yin et al., 2020), 100-m and 200-m Euclidean buffers of sampling points were generated in ArcGIS 10.2, and variables such as building density, floor area ratio (FAR), green area ratio and land use were calculated for each sampling point based on the association of buffers with green space and building footprint data.

For land use variables, the top four land use types in the study area, including residential communities, schools, urban parks, and shopping malls were selected, and the land area within 100-m and 200-m Euclidean buffers was calculated using ArcMap 10.2 separately.

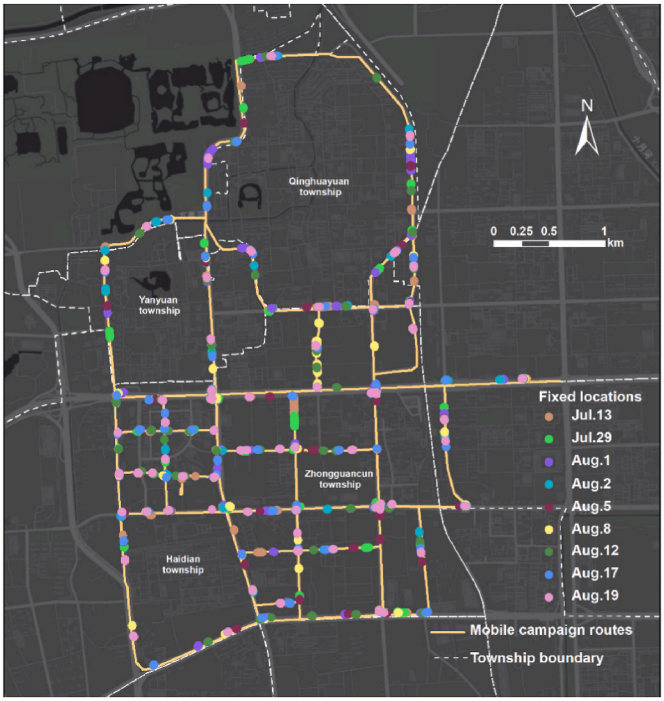

Fig. 3. Mobile routes and stationary sampling points in the RMM campaign.

For meteorological variables, $PM_{2.5}$, temperature and humidity

Fig. 4. Descriptions of the e-bike carrying professional monitoring devices.

value were directly extracted from the meteorological data, including timestamps and variable values at the moment of noise sensing.

2.5. Noise prediction modeling

Compared to linear regression (LN), machine learning methods are better able to address the multicollinearity issue and capture the potentially complex nonlinear relationships among variables. Therefore, this study trained six machine learning models using processed data and a total of 49 variables, including random forest regression (RF), K-nearest neighbors regression (KNN), gradient boosting regression (GB), decision tree regression (DT), support vector regression (SV) and Ada-boost regression (AR). For comparison, this study also trained the linear regression (LR) model. Meteorological, street form and traffic composition variables were added to the different models in steps to distinguish the role of different categories of variables in noise prediction. All the models were implemented using scikit-learn, the most useful machine learning package in Python. Grid search function was used to discover the optimized parameters for each regression model. A 10-fold cross-validation technique is utilized to partition the training and validation datasets.

2.6. Traffic noise mapping

In order to visualize the spatial and temporal heterogeneity of LAeq and generate noise maps with high spatial resolution, this study made predictions of LAeq during mobile monitoring. First, video, meteorological data and GPS coordinates were all recorded during the RMM, and based on these data all predictor variables at 1-s intervals (about 6-m spatial interval, which is equal to 1 s times the average speed of 20 km/h) were extracted according to the method above. Second, based on all models trained in the previous section, the model with the highest R^2 value was selected for prediction. In the last step, the predicted values of all points and street segments for each acquisition date were visualized in ArcGIS 10.2 software.

3. Results

3.1. Statistical summary

The sample size, and descriptions of the noise data for the 9 dates of the RMM campaign are presented in Table 3. The total number of measured traffic noise (N = 18,213) had a mean LAeq value of 68.3 dB, a standard deviation (SD) of 5.5 dB, and an interquartile range from 31.3 to 103.9 dB. The mean LAeq varied slightly by dates, ranging from 67.3 to 69.0 dB.

3.2. Model results

The performance of each model is shown in Table 4. Among the six machine learning models, five machine learning regression models showed better performance than the linear regression model, implying a complex nonlinear relationship between the predictor variables and the noise level. Among all the prediction models, the RF model performed the best, with a final R^2 of 0.72 and an RMSE of 3.28 dB, indicating that 72% of the data can be well explained with a deviation of 3.28 dB between the observed and true values. The KNN model also performed well with a final R^2 of 0.66 and an RMSE below 3.5 dB. The DT ($R^2 = 0.52$) and GB ($R^2 = 0.51$) models had acceptable performances, with R^2 above 0.5. In contrast, the performance of AR model was poor with a final R^2 of only 0.35. The SV and LR models performed the worst, with final R^2 of only 0.32 even when all predictor variables were included.

In the first step, only meteorological variables were included in the models, the R^2s of each model were low and did not exceed 0.6. Especially, the R^2s of SV ($R^2 = 0.01$), LR ($R^2 = 0.01$) and SV models ($R^2 = 0.06$) were all below 0.1. The KNN ($R^2 = 0.55$) and RF models ($R^2 = 0.51$) performed relatively well. Further inclusion of street form variables improved the model accuracy, and the RMSE of all models decreased. The RF ($R^2 = 0.66$) and KNN models (R2 = 0.61) performed well with final R^2s both above 0.6, while the LR and SV models still performed the worst ($R^2 = 0.29$). After including the traffic composition variables, except for the LR, SV and AR models, most models performed at acceptable levels, with final R^2s above 0.5.

Considering that the KNN model cannot calculate the relative contributions of the predictor variables, Table 5 showed the relative contributions of the top 10 predictor variables from the RF and DT models among the best 3 models. Overall, the street form variables had the highest contribution, exceeding 41% in the RF model and 39% in the DT model. The contribution of traffic composition variables exceeded 10% in both the RF and DT models. The contribution of meteorological variables was weak in both models. Humidity and temperature were the only two meteorological variables in the top 10 contribution list, with contributing the same of 6% to both the RF and GB models.

Although the predictor variables contribute differently to traffic noise in the two models, there were some similarities among the variables. The street form variables of distance to major road ranked first in both models, contributing 23% and 22% to the RF and GB models, respectively. The maximum view index of cars in the last 3 s, maximum

Table 3
Descriptive statistics for noise levels and sampling parameters.

Date	Sample	Minimum LAeq (db)	Maximum LAeq (db)	Average LAeq (db)	Std Error	Number of stationary sampling sites	Maximum sampling time (s)	Minimum sampling time (s)	Average sampling time (s)
July 13, 2022	2173	31.3	91.3	69.0	5.4	57	299	7	50.7
July 29, 2022	1841	52	98.3	67.7	5.7	46	113	10	42.1
August 1, 2022, July 13, 2022	2099	52	88.6	68.8	5.7	55	171	6	43.1
August 2, 2022	1803	49.2	103.9	69.3	5.7	51	288	12	47.4
August 5, 2022	1845	51.8	101.8	68.9	5.3	53	148	9	45.1
August 8, 2022	2178	53.5	97.5	67.5	5.1	53	122	14	46.8
August 12, 2022	2270	53.1	91.4	67.8	5.5	68	157	7	40.9
August 17, 2022	2108	47.8	102.7	68.2	5.7	61	145	10	40.8
August 19, 2022	1896	52	90.7	67.7	5.4	63	190	8	40.8
Total	18,213	31.3	103.9	68.3	5.5	152	299	6	44.0

Table 4
R^2 and RMSE of noise prediction models based on three types of variables.

Model covariates	Meteorological variables		+ Street form variables		+ Traffic composition variables	
	R^2	RMSE	R^2	RMSE	R^2	RMSE
Random forest (RF) regression	0.51	3.85	0.66	3.21	0.72	3.28
K-Nearest Neighbors (KNN) regression	0.55	3.70	0.61	3.18	0.66	3.43
Decision tree (DT) regression	0.40	4.26	0.42	4.18	0.52	4.89
Gradient Boosting (GB) regression	0.22	4.86	0.49	3.93	0.51	3.84
Adaboost regression (AR)	0.06	5.33	0.34	4.49	0.35	4.51
Support vector (SV) regression	0.01	5.48	0.29	4.62	0.32	4.53
Linear regression (LR)	0.01	5.46	0.29	4.63	0.32	4.50

view index of buses in the last 3 s and the tree view index ranked among the top five in both models, contributing 5%, 5% and 5% to the RF model and 5%, 5% and 4% to the GB model, respectively. The contribution of the remaining variables did not significantly vary, with none of them exceeding 5%.

Among them, the distance to the major-major intersection, distance to the major-secondary intersection, distance to the branch-branch intersection, humidity and temperature were among the top ten in both models, but with slightly differences at the contribution level. The distance to the major-secondary intersection contributed 4% in the RF model and 3% in the GB model. The distance to the branch-branch intersection contributed 4% in the GB model and 3% in the RF model.

Table 5
Relative contribution (RC) of predictor variables (Top 10) in top 2 models.

Model 1 Random forest regression	RC	Model 2 Decision tree regression	RC
Distance to the major road	23%	Distance to the major road	22%
Tree view index	5%	Maximum view index of cars	5%
Maximum view index of cars	5%	Maximum view index of buses	5%
Maximum view index of buses	5%	Distance to the branch-branch intersection	4%
Distance to the major-secondary intersection	4%	Tree view index	4%
Sky view index	3%	Humidity	3%
Humidity	3%	Distance to the major- major intersection	3%
Distance to the branch-branch intersection	3%	Land area of shopping mall within the 200-m Euclidean buffers	3%
Distance to the major-major intersection	3%	Distance to the major- secondary intersection	3%
Temperature	3%	Temperature	3%

The distance to the major-major intersection, humidity and temperature all contributed the same 3% to both models. In addition, some of these predictors were only among the top ten for one model. Sky view index contributed 3% in the RF model, while land area of shopping mall within the 200-m contributed 3% in the GB model.

3.3. Prediction maps

The optimal RF model was employed to predict traffic noise levels at both point and street scales along mobile monitoring routes. These predictions were combined with noise data from stationary sampling points to generate traffic noise maps over a period of nine days (see Figs. 5 and 6). It is important to note that the noise values at each coordinate point in the map corresponded to the LAeq values measured at the time of data collection, with a reference time of 1 s. Significant differences in noise levels were observed between different streets on the same day. For example, on August 17th, the mean LAeq value on streets was 69.3 dB, with values ranging from 64.9 to 73.7 dB. In addition, higher LAeq values were recorded on major and secondary roads and at intersections with high traffic volumes. Car honking at intersections also contributing to elevated traffic noise levels.

4. Discussion

To our knowledge, this is one of the earliest efforts combining mobile and stationary monitoring methods to collect noise data. In this study, a new noise monitoring method called Rotating Mobile Monitoring (RMM) method was proposed, and the noise data at random locations and intersections of approximate 54.79 km of roads in Beijing over a period of 9 days was collected. During the RMM campaign, both video data and meteorological data were collected. Microscopic traffic composition variables were extracted from the video data, land use and street form variables were measured from the built environment data and video data, all of which were considered as predictor variables for the noise prediction model, along with meteorological variables. Deep learning methods were deployed to construct our prediction models and to capture the complex nonlinear relationships between noise level and these variables at each second.

This study demonstrates the superiority of RMM, which can acquire accurate noise data over a large geographical area in a short period of time using less human labor. Compared to stationary monitoring (Mioduszewski et al., 2011; Zambon et al., 2018), RMM can collect traffic noise data at more locations (152 points in this study) with more spatial heterogeneity. The total area of our study is 22.15 km^2, which covers a wide mixture of different land uses, including commercial and business district, universities, residential communities, parks and roads at each grade. Compared to mobile monitoring (Quintero et al., 2021; Quintero et al., 2019), RMM is capable of acquiring relatively time-continuous noise data covering different traffic conditions, including transitions from few to many vehicles. More importantly, RMM does not need to

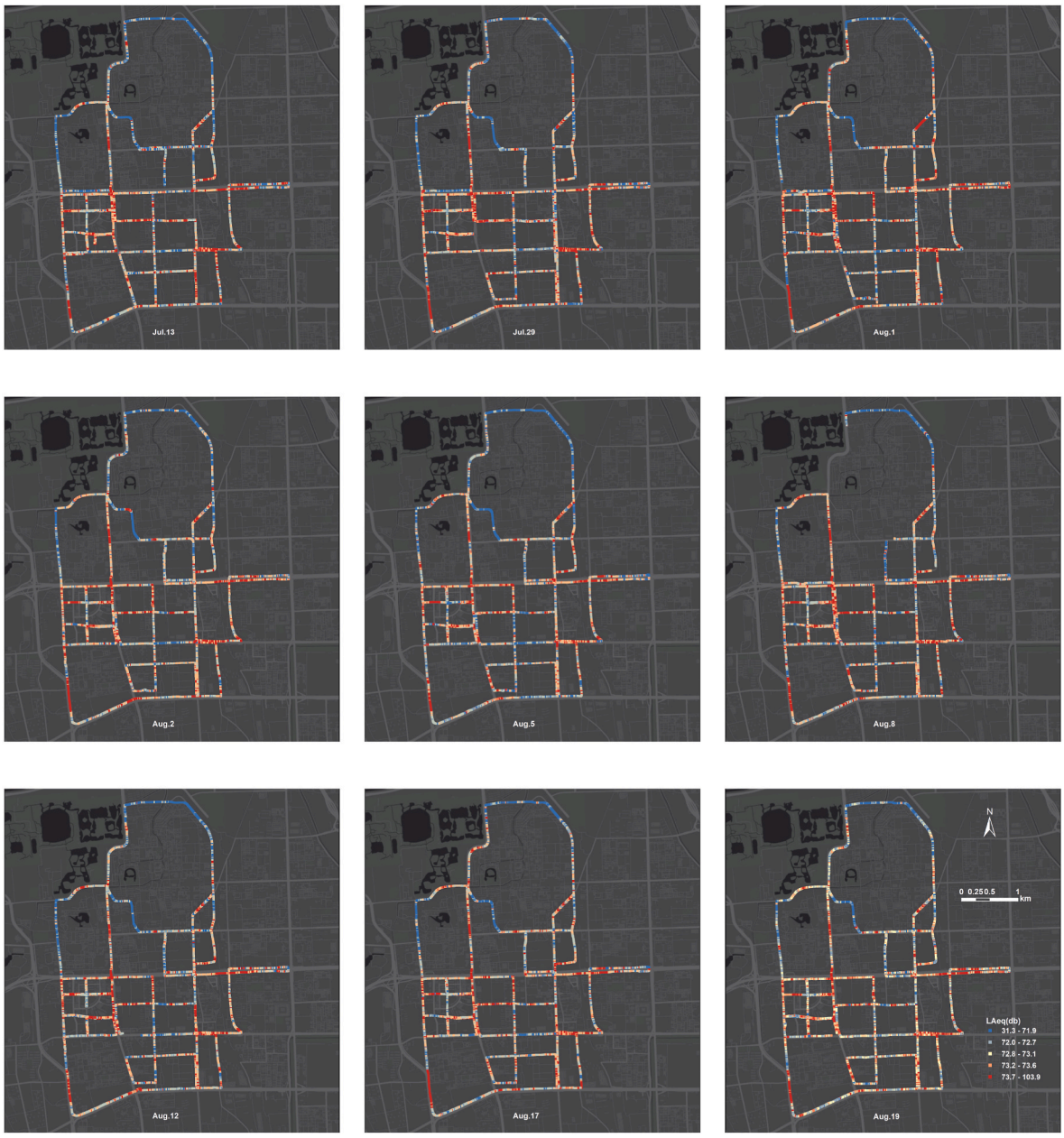

Fig. 5. Traffic noise distribution of the coordinate points for nine days.

consider the problem of noise levels being affected by movement, so it can cover a large geographical area in a short period of time. In our study, only one researcher was needed to collect traffic noise data for 55 km of road in less than 3 h. In the future, this method can be extended to other urban areas of Beijing.

In addition to noise data, video data and meteorological data were also collected in the RMM campaign, which could be used to measure predictor variables for microscopic traffic composition, built environment and meteorology. After examining the complex relationship between the predictor variables and the noise level, LAeq could be predicted for all the mobile routes, since the data used to measure the predictor variables covered the entire study area. Deep learning methods were applied to the construction of noise prediction models and the random forest model had the best performance with a final R^2 of 0.72 and an RMSE of 3.28 dB. In contrast, the linear regression model had the worst performance, with an R^2 of only 0.32, demonstrating the existence of a complex nonlinear relationship between the predictor variables and the noise level. In addition, the accuracy of our prediction models was improved compared to most previous studies. For example, Thakre et al. (2020) developed a noise prediction model using multiple regression analysis with a final R^2 of 0.64–0.65. The accuracy of our model was also improved compared to several studies that used deep learning models to predict traffic noise. Fallah-Shorshani et al. (2018) used land use regression to predict traffic noise with an R^2 of 0.44–0.64. Yin et al. (2020) developed several models to predict noise on 16 routes, including the neural network model (R^2: 0.44–0.75 (mean 0.61), RMSE: 3.34–7.93 dB (mean 4.89 dB)), the random forest model (R^2: 0.48–0.78 (mean 0.65), RMSE: 3.54–5.80 dB (mean 4.76 dB)) and the extreme gradient boosting model (R^2: 0.54–0.88 (mean 0.71), RMSE: 2.54–6.44 dB (mean 4.54 dB)).

Distance to the major road contributed the most to the prediction model in our study, which, to some extent, can reflect the level of traffic volume. Although this study is able to identify microscopic traffic volumes from video data, the videos were taken from the perspective of the human eye and cannot capture all vehicles on wider roads, so distance to the major road serves as a supplementary role.

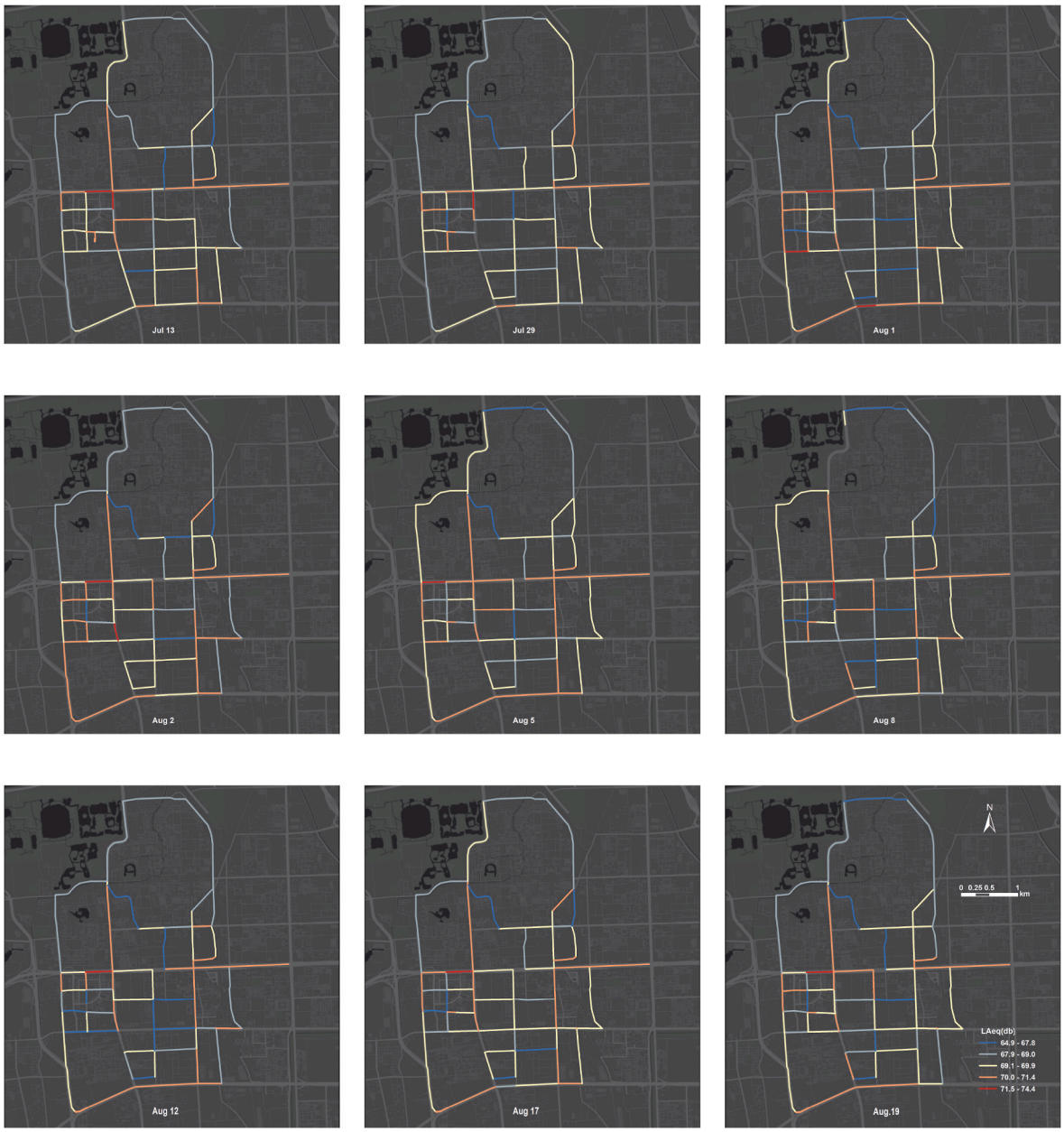

Fig. 6. Traffic noise distribution of street segments in nine days.

Most previous studies have confirmed that macroscopic traffic volume variable (average traffic flow within a certain time) is the strongest contributor in the model (Yin et al., 2020; Lee et al., 2014). However, microscopic traffic composition characteristics can reflect the actual traffic situation at a certain time and place, which corresponds to LAeq measured at 1-s intervals, and are more meaningful for highly dynamic traffic noise prediction. Our study confirms the crucial contribution of microscopic traffic composition characteristics in noise prediction models. In particular, the proportion of views of cars and buses is more important than their numbers, clarifying that the proportion representing the distance to the noise source is more important than the quantity. The prediction accuracy of RF model (R^2) was improved 6% after considering the traffic composition variables. Although Luca et al. (2021) and Sun et al. (2022) both considered using traffic composition characteristics that extracted from image data to predict traffic noise, they relied on image data provided by fixed location cameras, resulting in low spatial heterogeneity of noise sampling points. In addition, image-based deep learning models for traffic composition information extraction requires a large amount of labeled data for model training in a supervised manner (Luca et al., 2021). This study used the publicly available YOLOv7 model to process enormous image data for automated measurement of traffic composition variables, and the accuracy of this method has been demonstrated in the original studies (Wang et al., 2022). Meanwhile, the indispensable role played by image data in predicting noise levels should also be emphasized. In addition to microscopic traffic composition variables, the tree view and sky view indices with high relative contributions are also measured by image data. It can be concluded that LAeq with 1-s range can be accurately predicted by taking photographs on urban roads and knowing where the photographs were taken.

In summary, this study realizes the possibility of predicting highly dynamic traffic noise using RMM and machine learning methods, and generating high spatial resolution traffic noise maps from trained random forest model, which has a wide range of application scenarios in epidemiological studies, both to assess potential adverse health effects of individual-level traffic noise exposure and to account for noise as a

confounding effect in other traffic-related exposures such as air pollution (Yin et al., 2020). Although strategic noise maps have been used as a noise management tool in many European countries since the introduction of the Environmental Noise Directive. These strategic noise maps have some disadvantages: the prediction accuracy in shielded or quiet areas is not very high, and most importantly they did not consider dynamic traffic elements that could affect the acoustic environment (Wei et al., 2016). Our research makes it possible to monitor highly dynamic urban traffic noise and generate high spatial and temporal resolution noise maps using thousands of cameras within cities, so that streets and areas of severe noise pollution that require management control could be easily identified. Besides, since Google Street Views already cover most urban areas worldwide, these commercial street views can be used to map noise pollution for large geographical areas and identify inequalities in noise exposure for urban resident (Anguelov et al., 2010).

This study has several limitations that need to be acknowledged. Firstly, to ensure the safety of the data collectors and improve the collection efficiency, we chose to collect data only during off-peak hours from 12:00 to 16:00, which may not fully represent the noise pattern during peak traffic hours. Future studies will need to investigate the noise pattern during peak hours to provide a more comprehensive understanding of traffic noise. Second, traffic conditions such as airports were not addressed in the study area. Third, this study only collected data in Beijing, and the transferability of the model is unknown. Experimental validation in other cities will be conducted in the future. Finally, as previous studies have demonstrated that spatial variation in noise is more important than temporal variation, our study focused on various noise sources but was unable to capture well the temporal trend. However, it gave us insight that in the future, the use of stabilization time (ST) (Brambilla et al., 2022) can be employed to analyze and determine a statistically representative sample of the urban acoustic environment, thereby enhancing the representativeness of the noise map over time.

5. Conclusion

In this study, a new traffic noise monitoring method, Rotating Mobile Monitoring method (RMM), is proposed, and it is demonstrated that this method can combine the advantages of stationary and mobile monitoring methods to achieve the collection of high-precision large-scale noise data with high spatial and temporal resolution but with less labor and time. A total of 18,213 LAeq samples at 1-s intervals were obtained from 152 stationary locations during the nine-day RMM campaigns. For predicting LAeq, the Random Forest model performed best ($R^2 = 0.72$, RMSE = 3.28 dB), followed by the K-Nearest Neighbors regression model ($R^2 = 0.66$, RMSE = 3.43 dB), which was substantially more accurate than the linear regression model and demonstrated the complex nonlinear relationship between predictor variables and traffic noise. In the RF models, distance to the major road, tree view index and the maximum view index of cars in the last 3 s are the three most important predictors of traffic noise, with a total contribution of 33%. Most importantly, our study confirms the important role of microscopic traffic composition variables in predicting traffic noise, which offers great possibilities for constructing highly dynamic noise maps. Also using our trained model, the images can be used to accurately predict traffic noise after knowing where the images were taken, which has important practical implications for noise management.

Credit author statement

Yuyang Zhang: Conceptualization; Methodology; Formal analysis; Writing – original draft; Writing – review & editing. Huimin Zhao: Visualization; Writing – original draft; Writing – review & editing. Yan Li: Data curation; Methodology; Formal analysis; Writing – original draft; Writing – review & editing; Supervision. Ying Long: Conceptualization; Writing – review & editing. Weinan Liang: Writing – review & editing.

Declaration of competing interest

The authors declare that they have no known competing financial interests or personal relationships that could have appeared to influence the work reported in this paper.

Data availability

Data will be made available on request.

Acknowledgements

This work was supported by Chinese National Postdoctoral Foundation [2019TQ0166]. The authors would like to thank Junyan Zhang for supporting the research.

References

Ahmed, A.A., Pradhan, B., 2019. Vehicular traffic noise prediction and propagation modelling using neural networks and geospatial information system. Environ. Monit. Assess. 191 (3), 1–17. https://doi.org/10.1007/s10661-019-7333-3.

Anguelov, D., Dulong, C., Filip, D., Frueh, C., Lafon, S., Lyon, R., Ogale, A., Vincent, L., Weaver, J., 2010. Google street view: capturing the world at street level. Computer 43 (6), 32–38. https://doi.org/10.1109/MC.2010.170.

Begou, P., Kassomenos, P., Kelessis, A., 2020. Effects of Road Traffic Noise on the Prevalence of Cardiovascular Diseases: the Case of Thessaloniki, Greece, vol. 703. Science of the total environment, 134477. https://doi.org/10.1016/j.scitotenv.2019.134477.

Brambilla, G., Benocci, R., Potenza, A., Zambon, G., 2022. Stabilization time of running equivalent level LAeq for urban road traffic noise. Appl. Sci. 13 (1), 207. https://doi.org/10.3390/app13010207.

Chang, T.Y., Liang, C.H., Wu, C.F., Chang, L.T., 2019. Application of Land-Use Regression Models to Estimate Sound Pressure Levels and Frequency Components of Road Traffic Noise in Taichung, Taiwan, vol. 131. Environment international, 104959. https://doi.org/10.1016/j.envint.2019.104959.

Chen, L., Tang, B., Liu, T., Xiang, H., Sheng, Q., Gong, H., 2020. Modeling traffic noise in a mountainous city using artificial neural networks and gradient correction. Transport. Res. Transport Environ. 78, 102196 https://doi.org/10.1016/j.trd.2019.11.025.

Clark, S.N., Alli, A.S., Ezzati, M., Brauer, M., Toledano, M.B., Nimo, J., Moses, J.B., Baah, S., Hughes, A., Cavanaugh, A., Agyei-Mensah, S., 2022. Spatial Modelling and Inequalities of Environmental Noise in Accra, Ghana, vol. 214. Environmental research, 113932. https://doi.org/10.1016/j.envres.2022.113932.

Fallah-Shorshani, M., Minet, L., Liu, R., Plante, C., Goudreau, S., Oiamo, T., Smargiassi, A., Weichenthal, S., Hatzopoulou, M., 2018. Capturing the spatial variability of noise levels based on a short-term monitoring campaign and comparing noise surfaces against personal exposures collected through a panel study. Environ. Res. 167, 662–672. https://doi.org/10.1016/j.envres.2018.08.021.

Fallah-Shorshani, M., Yin, X., McConnell, R., Fruin, S., Franklin, M., 2022. Estimating Traffic Noise over a Large Urban Area: an Evaluation of Methods, vol. 170. Environment international, 107583. https://doi.org/10.1016/j.envint.2022.107583.

Garg, N., Maji, S., 2014. A critical review of principal traffic noise models: strategies and implications. Environ. Impact Assess. Rev. 46, 68–81. https://doi.org/10.1016/j.eiar.2014.02.001.

Gebru, T., Krause, J., Wang, Y., Chen, D., Deng, J., Aiden, E.L., Fei-Fei, L., 2017. Using deep learning and Google Street View to estimate the demographic makeup of neighborhoods across the United States. Proc. Natl. Acad. Sci. USA 114 (50), 13108–13113. https://doi.org/10.1073/pnas.1700035114.

Genaro, N., Torija, A., Ramos-Ridao, A., Requena, I., Ruiz, D.P., Zamorano, M., 2010. A neural network based model for urban noise prediction. J. Acoust. Soc. Am. 128 (4), 1738–1746. https://doi.org/10.1121/1.3473692.

Ghosh, A., Kumari, K., Kumar, S., Saha, M., Nandi, S., Saha, S., 2019. Noiseprobe: assessing the dynamics of urban noise pollution through participatory sensing. January. In: 2019 11th International Conference on Communication Systems & Networks (COMSNETS). IEEE, pp. 451–453. https://doi.org/10.1109/COMSNETS.2019.8711473.

Gilani, T.A., Mir, M.S., 2021. Modelling road traffic Noise under heterogeneous traffic conditions using the graph-theoretic approach. Environ. Sci. Pollut. Res. 28 (27), 36651–36668. https://doi.org/10.1007/s11356-021-13328-4.

Guillaume, G., Aumond, P., Chobeau, P., Can, A., 2019. Statistical study of the relationships between mobile and fixed stations measurements in urban environment. Build. Environ. 149, 404–414. https://doi.org/10.1016/j.buildenv.2018.12.014.

Halfwerk, W., Holleman, L.J., Lessells, C.K.M., Slabbekoorn, H., 2011. Negative impact of traffic noise on avian reproductive success. J. Appl. Ecol. 48 (1), 210–219. https://doi.org/10.1111/j.1365-2664.2010.01914.x.

Ibili, F., Owolabi, A.O., 2019. Replication of calculation of road traffic noise model for traffic noise prediction at the central business district of Ondo Town, Nigeria. J. Geotech. Trans. Eng. 5 (1).

Kang, Y., Zhang, F., Gao, S., Lin, H., Liu, Y., 2020. A review of urban physical environment sensing using street view imagery in public health studies. Spatial Sci. 26 (3), 261–275. https://doi.org/10.1080/19475683.2020.1791954.

Kanjo, E., 2010. Noisespy: a real-time mobile phone platform for urban noise monitoring and mapping. Mobile Network. Appl. 15 (4), 562–574. https://doi.org/10.1007/s11036-009-0217-y.

Klompmaker, J.O., Hoek, G., Bloemsma, L.D., Wijga, A.H., van den Brink, C., Brunekreef, B., Lebret, E., Gehring, U., Janssen, N.A., 2019. Associations of combined exposures to surrounding green, air pollution and traffic noise on mental health. Environ. Int. 129, 525–537. https://doi.org/10.1016/j.envint.2019.05.040.

Lan, Z., Cai, M., 2021. Dynamic traffic noise maps based on noise monitoring and traffic speed data. Transp. Res. Part D Transp. Environ. *94*, 102796. https://doi.org/10.1016/j.trd.2021.102796.

Lan, Y., Roberts, H., Kwan, M.P., Helbich, M., 2020. Transportation noise exposure and anxiety: a systematic review and meta-analysis. Environ. Res. 191, 110118 https://doi.org/10.1016/j.envres.2020.110118.

Leao, S., Ong, K.L., Krezel, A., 2014. 2Loud?: community mapping of exposure to traffic noise with mobile phones. Environ. Monit. Assess. 186 (10), 6193–6206. https://doi.org/10.1007/s10661-014-3848-9.

Lee, E.Y., Jerrett, M., Ross, Z., Coogan, P.F., Seto, E.Y., 2014. Assessment of traffic-related noise in three cities in the United States. Environ. Res. 132, 182–189. https://doi.org/10.1016/j.envres.2014.03.005.

Liptai, P., Badida, M., Lukáčová, K., 2015. Influence of atmospheric conditions on sound propagation-mathematical modeling. Óbuda Univ. e-Bull. 5 (1), 127. https://www.researchgate.net/publication/289525229_Influence_of_Atmospheric_Conditions_on_Sound_Propagation_-_Mathematical_Modeling.

Lu, H., Pan, W., Lane, N.D., Choudhury, T., Campbell, A.T., 2009. Soundsense: scalable sound sensing for people-centric applications on mobile phones. In: *Proceedings of the 7th international conference on Mobile systems, applications, and services*, pp. 165–178. https://doi.org/10.1145/1555816.1555834.

Lu, X., Kang, J., Zhu, P., Cai, J., Guo, F., Zhang, Y., 2019. Influence of urban road characteristics on traffic noise. Transport. Res. Transport Environ. 75, 136–155. https://doi.org/10.1016/j.trd.2019.08.026.

Mansourkhaki, A., Berangi, M., Haghiri, M., Haghani, M., 2018. A neural network noise prediction model for Tehran urban roads. J. Environ. Eng. Landsc. Manag. 26 (2), 88–97. https://doi.org/10.3846/16486897.2017.1356327.

Mioduszewski, P., Ejsmont, J.A., Grabowski, J., Karpiński, D., 2011. Noise map validation by continuous noise monitoring. Appl. Acoust. 72 (8), 582–589. https://doi.org/10.1016/j.apacoust.2011.01.012.

Monti, L., Vincenzi, M., Mirri, S., Pau, G., Salomoni, P., 2020. Raveguard: a noise monitoring platform using low-end microphones and machine learning. Sensors 20 (19), 5583. https://doi.org/10.3390/s20195583.

Morel, J., Marquis-Favre, C., Dubois, D., Pierrette, M., 2012. Road traffic in urban areas: a perceptual and cognitive typology of pass-by noises. Acta Acustica united Acustica 98 (1), 166–178. https://doi.org/10.3813/AAA.918502.

Nijland, H.A., Van Wee, G.P., 2005. Traffic noise in Europe: a comparison of calculation methods, noise indices and noise standards for road and railroad traffic in Europe. Transport Rev. 25 (5), 591–612. https://doi.org/10.1080/01441640500115850.

Nourani, V., Gökçekuş, H., Umar, I.K., Najafi, H., 2020. An emotional artificial neural network for prediction of vehicular traffic noise. Sci. Total Environ. 707, 136134. https://doi.org/10.1016/j.scitotenv.2019.136134.

Paiva, K.M., Cardoso, M.R.A., Zannin, P.H.T., 2019. Exposure to road traffic noise: annoyance, perception and associated factors among Brazil's adult population. Sci. Total Environ. 650, 978–986. https://doi.org/10.1016/j.scitotenv.2018.09.041.

Quintero, G., Aumond, P., Can, A., Balastegui, A., Romeu, J., 2019. Statistical requirements for noise mapping based on mobile measurements using bikes. Appl. Acoust. 156, 271–278. https://doi.org/10.1016/j.apacoust.2019.07.020.

Quintero, G., Balastegui, A., Romeu, J., 2021. Traffic noise assessment based on mobile measurements. Environ. Impact Assess. Rev. 86, 106488 https://doi.org/10.1016/j.eiar.2020.106488.

Ryu, H., Park, I.K., Chun, B.S., Chang, S.I., 2017. Spatial statistical analysis of the effects of urban form indicators on road-traffic noise exposure of a city in South Korea. Appl. Acoust. 115, 93–100. https://doi.org/10.1016/j.apacoust.2016.08.025.

Sørensen, M., Poulsen, A.H., Hvidtfeldt, U.A., Brandt, J., Frohn, L.M., Ketzel, M., Christensen, J.H., Im, U., Khan, J., Münzel, T., Raaschou-Nielsen, O., 2022. Air pollution, road traffic noise and lack of greenness and risk of type 2 diabetes: a multi-exposure prospective study covering Denmark. Environ. Int. 170, 107570 https://doi.org/10.1016/j.envint.2022.107570.

Shukla, S.P., Yadav, S.K., Lohani, B., Biswas, S., Behra, S.N., Singh, N.B., Singh, N.K., 2012. Characterization of traffic noise for a typical Indian road crossing. Curr. Sci. 1193–1201. http://www.jstor.org/stable/24089232.

Sun, Y., Wu, M., Liu, X., Zhou, L., 2022. High-precision dynamic traffic noise mapping based on road surveillance video. ISPRS Int. J. Geo-Inf. 11 (8), 441. https://doi.org/10.3390/ijgi11080441.

Thakre, C., Laxmi, V., Vijay, R., Killedar, D.J., Kumar, R., 2020. Traffic noise prediction model of an Indian road: an increased scenario of vehicles and honking. Environ. Sci. Pollut. Res. 27 (30), 38311–38320. https://doi.org/10.1007/s11356-020-09923-6.

Wang, C.-Y., Bochkovskiy, A., Liao, H.-Y.M., 2022. YOLOv7: Trainable Bag-Of-Freebies Sets New State-Of-The-Art for Real-Time Object Detectors arXiv preprint arXiv: 2207.02696.

Wang, T.C., Chang, T.Y., Tyler, R.S., Hwang, B.F., Chen, Y.H., Wu, C.M., Liu, C.S., Chen, K.C., Lin, C.D., Tsai, M.H., 2021. Association between exposure to road traffic noise and hearing impairment: a case-control study. J. Environ. Health Sci. Eng. 19 (2), 1483–1489. https://doi.org/10.1007/s40201-021-00704-y.

Wei, W., Van Renterghem, T., De Coensel, B., Botteldooren, D., 2016. Dynamic noise mapping: a map-based interpolation between noise measurements with high temporal resolution. Appl. Acoust. 101, 127–140. https://doi.org/10.1016/j.apacoust.2015.08.005.

Yan, Y., Ryu, Y., 2021. Exploring Google Street View with deep learning for crop type mapping. ISPRS J. Photogrammetry Remote Sens. 171, 278–296. https://doi.org/10.1016/j.isprsjprs.2020.11.022.

Yin, X., Fallah-Shorshani, M., McConnell, R., Fruin, S., Franklin, M., 2020. Predicting fine spatial scale traffic noise using mobile measurements and machine learning. Environ. Sci. Technol. 54 (20), 12860–12869. https://doi.org/10.1021/acs.est.0c01987.

Zambon, G., Roman, H.E., Smiraglia, M., Benocci, R., 2018. Monitoring and prediction of traffic noise in large urban areas. Appl. Sci. 8 (2), 251. https://doi.org/10.3390/app8020251.

Zappatore, M., Longo, A., Bochicchio, M.A., 2016. Using mobile crowd sensing for noise monitoring in smart cities. July. In: 2016 International Multidisciplinary Conference on Computer and Energy Science (Splitech). IEEE, pp. 1–6. https://doi.org/10.1109/SpliTech.2016.7555950.

Zhang, Y., Liu, N., Li, Y., Long, Y., Baumgartner, J., Adamkiewicz, G., Gemmell, E., 2023. Neighborhood infrastructure-related risk factors and non-communicable diseases: a systematic meta-review. Environmental Health 22 (1), 1–15.